Ultrashort pulsed fiber laser welding and sealing of transparent materials

Huan Huang,* Lih-Mei Yang, and Jian Liu

PolarOnyx, Inc., 2526 Qume Drive, Suite 17 & 18, San Jose, California, 94538, USA

*Corresponding author: hhuang@polaronyx.com

Received 31 October 2011; revised 8 February 2012; accepted 15 February 2012;
posted 15 February 2012 (Doc. ID 157363); published 18 May 2012

In this paper, methods of welding and sealing optically transparent materials using an ultrashort pulsed (USP) fiber laser are demonstrated which overcome the limit of small area welding of optical materials. First, the interaction of USP fiber laser radiation inside glass was studied and single line welding results with different laser parameters were investigated. Then multiline scanning was used to obtain successful area bonding. Finally, complete four-edge sealing of fused silica substrates with a USP laser was demonstrated and the hermetic seal was confirmed by water immersion test. This laser microwelding technique can be extended to various applications in the semiconductor industry and precision optic manufacturing. © 2012 Optical Society of America

OCIS codes: 140.3390, 140.7090.

1. Introduction

Joining and welding of optical transparent materials is required for many applications, such as life science, sensing, optoelectronics, and MEMS packaging. Current joining methods are developed with specific properties that make them useful with limited applications. Joining technologies, such as binding or gluing using adhesives, suffer from mismatch between the thermal expansion coefficients of material and the adhesive, and the long-term stability of the bonds [1]. Oxygen and moisture gradually penetrate the interior of the component and affect its function. The limited durability and the temperature sensitivity of glued connections are the major problems, especially for components used in the medical sector. The most common bonding technique for glasses is optical contact. This is an adhesive-free process by which two ultraflat and ultraclean surfaces with the same curvature are bound together by the molecular attraction between the surface atoms [2]. However, the bond strength is typically very weak (a few kilopascals) and is highly susceptible to impact load. Laser welding using continuous wave lasers or long pulsed lasers has problems with crack development during the cooling period [3–5]. Moreover, since it is based on linear absorption, it requires one of the samples to be joined to be transparent and the other sample to be absorbing at the wavelength of the lasers used. The selection of materials to be joined is limited and it cannot be carried out for nonabsorbing materials such as glasses.

Alternatively, ultrashort (USP) lasers have been emerging as a promising tool in microfabrication [6,7] and biomedical applications [8,9], owing to their unique nonthermal interaction mechanisms with materials. They can also be used to induce local modifications inside the bulk of transparent materials due to nonlinear absorption, and this has been utilized for fabrication of waveguide and active integrated optical devices [10–13]. When the USP laser pulses are tightly focused, the high intensity inside the focal volume will induce multiphoton or tunneling ionization and subsequent avalanche ionization. Finally, this nonlinear absorption results in the creation of hot plasma and subsequent heating to the surrounding materials. Therefore, the USP laser can act as a local heat source in the volume and lead to melting of the materials. The melting and

1559-128X/12/152979-08$15.00/0

quenching of the material result in the generation of covalent bonds if the laser focus is located at the interface between two adjacent samples. The joining of transparent materials using USP lasers has been demonstrated by many researchers for both similar materials [14–22] and dissimilar materials [18,19,23]. USP laser joining allows space-selective joining without inserting intermediate layers, and the highly localized heat generation minimizes the thermal induced stress and can effectively suppress the development of thermally induced cracks. It also shows that high repetition rate laser systems operating in the megahertz range can lead to an enlarged modification region due to heat accumulation of successive pulses [16]. However, there are still problems in this research, such as small area welding between substrates or components, slow processing speed, and crack development, that limit the usage for industrial applications. Furthermore, most of the research results are based on solid state lasers. Fiber laser systems have the advantages of being compact, stable, reliable, and low cost and, more importantly, they can provide a high repetition rate and thus can increase the processing speed for future industrial applications.

In this paper, the interaction of USP fiber laser radiation inside glass was investigated first after single line scanning with 1030 nm and 750 fs pulse duration. Then two transparent glass substrates were welded with a USP laser by single line and multiline scanning. Finally, complete four-edge sealing of two glass substrates was demonstrated with a 10 mm^2 welding area size. This greatly increases the potential for USP laser welding applications in the semiconductor industry, precision optics manufacturing, and aerospace engineering.

2. Experimental Setup and Materials

The schematic of the USP laser welding experimental setup is shown in Fig. 1. The USP laser system is a commercialized mode-locked fiber laser manufactured by PolarOnyx, Inc. The output beam is typically Gaussian shaped with a pulse width of 750 fs and center wavelength of 1030 nm. The pulse repetition rate is tunable between 1 Hz and 1 MHz with the help of an acousto-optic modulator (AOM). The maximum output pulse energy is 5 μJ. The laser beam is reflected by mirrors and focused by an objective lens towards the sample on the sample fixture. Since direct measurement of the focal spot size was not feasible; an estimation of the smallest value of focal spot diameter is used by Eq. (1):

$$D = 1.22\frac{\lambda}{\text{N.A.}}, \tag{1}$$

where λ is the laser wavelength and N.A. is the numerical aperture of the objective lens. Two kinds of objective lens were used (N.A. = 0.4 and 0.55) and the focal spot diameters both are less than 5 μm. The total loss of the beam delivery system is less than 50%. Such a loss has been accounted for in the irradiation pulse energy values stated hereafter. An attenuator is used to control the laser pulse energy for fabrication, and a mechanical shutter is synchronized with the laser system. A CCD camera is placed along the optical axis and used to align the sample and obtain a live view for the laser processing.

The motion system includes an automated high-accuracy one-dimensional (x axis) linear stage with 50 mm travel range and 350 mm/s maximum speed, and two manually controlled linear stages for the other two other axes (y and z axes). Furthermore, the sample fixture has two tilt angle adjustments for sample tilting and alignment. A mechanical mount was used to clamp the sample substrates with pressure. Figure 2 shows a cross section of the sample fixture with the laser beam direction. Two transparent material substrates are stacked together and a cylindrical lens that creates a pressure region under the bottom plate is placed underneath the bottom substrate. Moderate pressure was applied on both top and bottom plates, and close contact was achieved at the interface of the two sample substrates. The laser beam was irradiated from the top, through the open window of the top plate. A cylindrical lens, or portion of a cylinder, will create a linear pressure region between the two substrates. A cushion material on top of the cylindrical lens was used to extend the pressure area and to keep the pressure uniform over the area. By using an

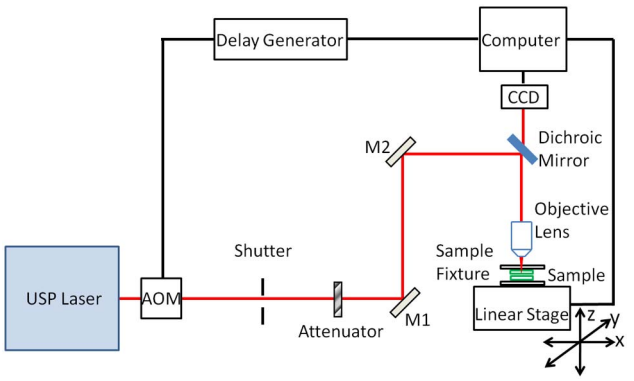

Fig. 1. (Color online) Experimental set up for USP laser welding and sealing of transparent materials.

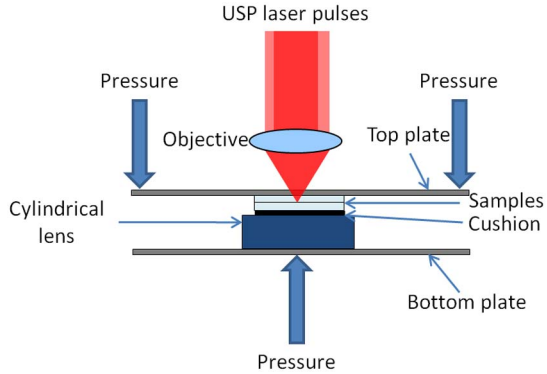

Fig. 2. (Color online) Sketch of cross section of the fixture for USP laser welding and sealing.

extended pressure region, it is possible to weld longer lengths and subsequently larger total areas; meanwhile, it can also prevent the overstressing or fracturing of the bottom substrate. The sample is moved together with the linear stage and the focused laser beam is irradiated from the top in transverse direction. The linear motion stage and the delay generator for the AOM are controlled by computer to achieve different sample moving speeds and different pulse repetition rates.

In this experiment, fused silica (Corning 7980) was used since fused silica has excellent mechanical, electrical, chemical, and especially optical properties, and is widely used in numerous applications such as optics, telecommunications, electronics, MEMS, and biomedicine. The fused silica sample dimension was 10 mm × 10 mm, with a thickness of 0.5 or 1 mm. To avoid ablation and ensure successful welding, the sample substrates have to be finely polished. The surface of the sample is 2 nm and the flatness is around 1/4 wave per inch across the surface. Before processing, each sample was cleaned by isopropanol.

The microtopography of the modification by USP laser was characterized with an upright digital microscope (ME520T-9M), and the cross section of the modification was checked after polishing both edges. The welding seam and region were checked and measured by scanning electron microscopy (SEM; FEI QUANTA FEG 600).

3. Experimental Results

The size and shape of the molten region depends on the laser parameters and the sample translation velocity. To systematically study the USP laser modification inside the material, the sample was scanned at speeds from 0.5 to 20 mm/s, pulse energies ranging from 100 nJ to 5 μJ, N.A. of 0.40 or 0.55, and a 1 MHz repetition rate. A cross section for a typical thermally induced modification shape inside fused silica is shown in Fig. 3. The laser beam is irradiated from the top (N.A. = 0.55) and each line was scanned only once with the same depth of 200 μm. For all the USP laser modification areas, as shown in Fig. 3, the laser pulse energies used from left to right are 0.45, 0.37, 0.25, 0.21, and 0.16 μJ, respectively, and the scanning speeds are the same −0.5 mm/s.

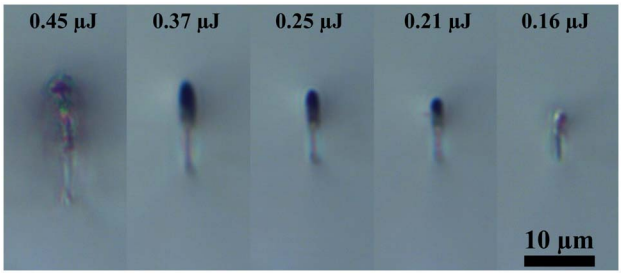

Fig. 3. (Color online) Microscopic view of cross sections of the fused silica modification region by USP laser with different pulse energies and the same speed (0.5 mm/s).

Since the repetition rate is high and there are hundreds of thousands of pulses hitting at the same spot, a useful measurement of exposure is the average fluence F_{ave} along the writing path, and it can be defined by Eq. (2):

$$F_{\text{avg}} = \frac{E * R}{D * v}, \tag{2}$$

where E is the single pulse energy, R is the repetition rate, and v is the laser writing speed. The average fluences used in Fig. 3 are 39.1, 32.1, 21.7, 18.2, and 13.9 kJ/cm^2, from left to right. As shown in Fig. 3, the laser-modified region shows a double structure, a center core with a droplet-like surrounding volume. This can be interpreted by considering the inner core as the directly irradiated focal region and the outer structure as the region modified due to the heat accumulation. By increasing the pulse energy at a constant translation speed, the overall modified volume width and depth also increases. For 0.5 mm/s writing speed, the minimum energy for the visible modified area is 0.10 μJ (F_{ave} = 8.7 kJ/cm^2) and no melt occurs in the material surrounding the focal volume for lower pulse energy. For higher writing speed, the minimum energy for the visible modified area is higher.

For USP laser welding, the laser focus was positioned at the interface between the two fused silica substrates. First of all, single line welding was conducted with different laser parameters. After processing, the welded samples were broken apart to study and characterize the welded region. Figure 4 shows the microscopic view of single-line welding results at the bottom fused silica substrate after being broken apart with different welding speeds and the same pulse energy (0.95 μJ, N.A. = 0.4). Both of the sample dimensions are 10 mm × 10 mm with 1.0 mm thickness. The welding speeds are 0.1, 0.2, 0.5, 1.0, and 2.0, respectively, from top to bottom. It is noted that the welding seams with speeds from 0.5 to 5.0 mm/s are not continuous. This is because

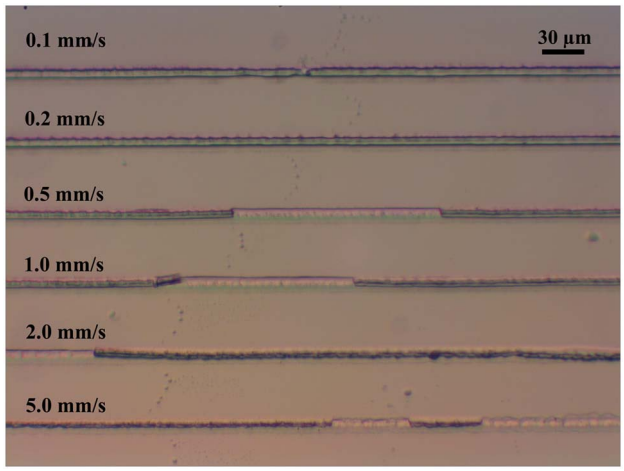

Fig. 4. (Color online) Microscopic view of single line welding at the bottom fused silica substrate with different scanning speeds and the same pulse energy (0.95 μJ).

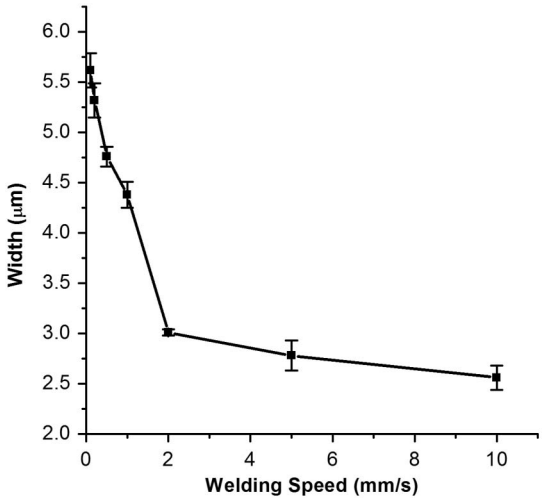

Fig. 5. Single line welding widths for different welding speeds and the same pulse energy (0.95 μJ).

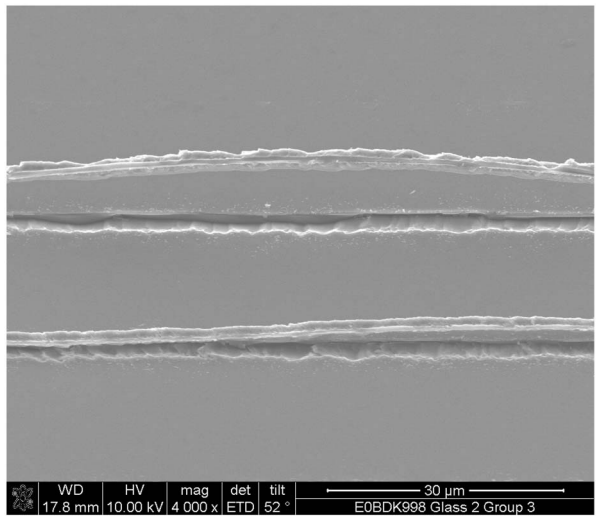

Fig. 7. SEM enlarged view of bottom substrate surface with single line welding after broken apart ($F_{ave} = 26.5$ kJ/cm^2).

portions of the seams remained at the top substrate when broken apart. Figure 5 shows the measured single-line welding seam widths for different welding speeds shown in Fig. 4. As shown in Fig. 5, the single-line welding seam width decreases from 5.6 to 2.6 μm when the welding speed is increased from 0.1 mm/s to 10 mm/s. Although the weld line width becomes smaller for larger scanning speeds, the welding seam is still kept uniform. High speed welding and sealing makes the welding technique applicable for industrial applications. The welding seam width and strength can be compensated for by using higher pulse energy or higher repetition rates.

Figure 6 shows the SEM tilted angle view of the single-line welding of another set of fused silica substrates after being broken apart. Both of the sample dimensions are 10 mm × 10 mm with 0.5 mm thickness. The welding speed is 1 mm/s and the average fluence used here is 26.5 kJ/cm^2. Figure 6(a) shows the welding surface of the top substrate showing grooves (the welding seam peeled off), and Fig. 6(b) shows the welding surface of the bottom substrate showing bumps (the welding seam remains). So the single-line welding seam can be clearly seen, and most of the welding seam remains on the bottom substrate since the bottom substrate is fixed and the top substrate is peeled off manually. Figure 7 shows an enlarged SEM view of the welding seam that remained on the bottom substrate shown in Fig. 6(b), and it clearly shows that part of the welding seam is above the substrate.

After the single-line welding experiment, multiline welding experiments were also conducted in order to obtain a large welding area. Space was properly chosen for the overlapping between scanning lines. Figure 8 shows the SEM view of the multiline welded region after being broken apart. Both of the sample substrate dimensions are 10 mm × 10 mm with 0.5 mm thickness. The welding speed is 1 mm/s and the average fluence used here is 26.5 kJ/cm^2. Figures 8(a) and 8(b) illustrate the same welded

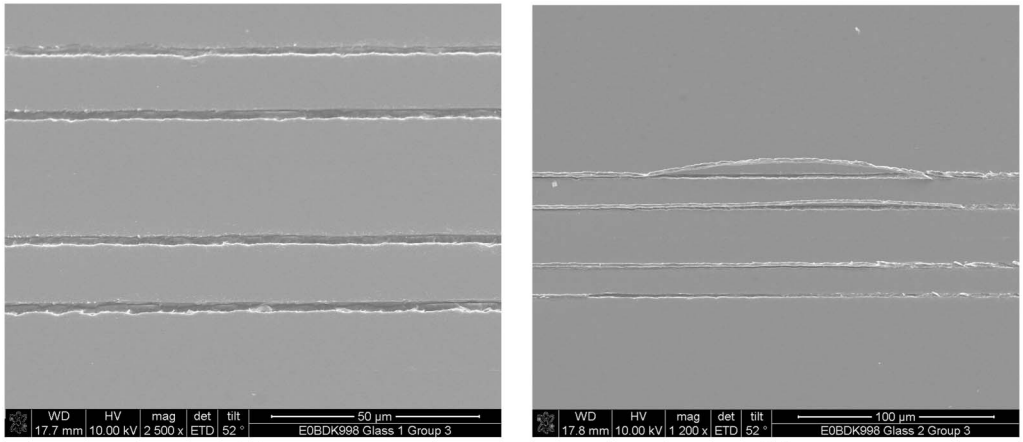

Fig. 6. SEM tilted angle view of single line welding of fused silica after broken apart ($F_{ave} = 26.5$ kJ/cm^2): (a) the welding surface of the top substrate showing grooves welding seam peeled off, and (b) the welding surface of the bottom substrate showing bumps welding seam remains.

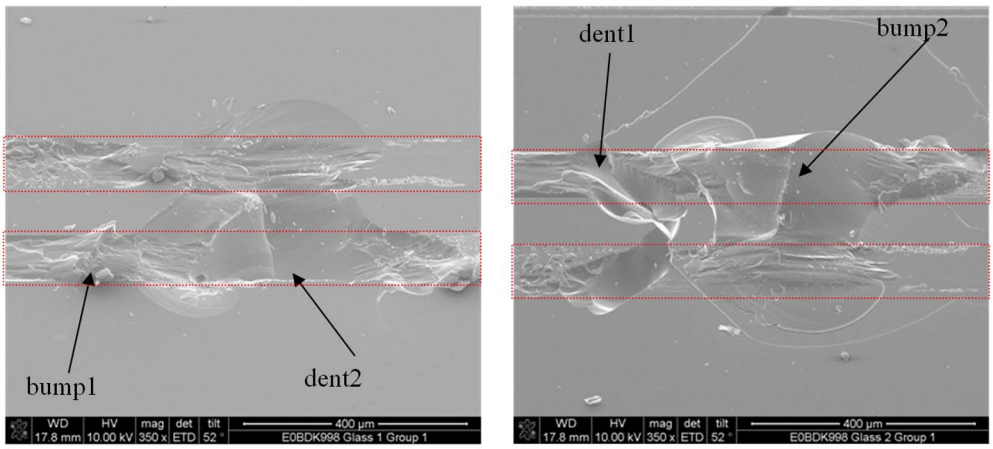

Fig. 8. (Color online) SEM tilted angle view of multiline welding region of fused silica ($F_{ave} = 26.5$ kJ/cm^2) after broken apart: (a) the welding surface of the top substrate, and (b) the welding surface of the bottom substrate.

region on the two substrate surfaces; Fig. 8(a) shows the welding surface of the top substrate and Fig. 8(b) shows the welding surface of the bottom substrate. For both surfaces, there are two welding areas (highlighted by the two red squares), and each area is composed of 20 welding lines with a 5 μm space. Each area was scanned three times to strengthen the bond. As shown in Fig. 8, dents and bumps of various sizes can be found on both substrate surfaces. The size of the dent on one surface corresponds to the size of the bump on the other surface. The one-to-one corresponding dents and bumps show the welding effects of the two substrates. It should be pointed out that, for the larger bump, some of the middle section between the two welded areas was peeled off without laser processing due to a bonding effect.

Figure 9 illustrates laser–glass one-edge sealing with multiline welding. Both sample dimensions are 10 mm × 10 mm with 1 mm thickness. The welded line starts from one edge of the sample to the end of the other edge, and each of the welding lines is 10 mm long. From the camera picture shown in this figure, there is clearly a rectangular section (black rectangular region) that does not show any interference fringe all the way along the sample from left to right. This shows very good, complete one-edge sealing along the whole length. For the welded region, there are two totally welded area sections; each section is about 500 μm wide with 5 μm pitches, and the welding speed was 1 mm/s. From top to bottom, the first section was scanned two times with average fluence of 37.4 kJ/cm^2 and 10 μm focal position change; the sample moves towards the laser beam. The second section was scanned three times with average fluence of 27.0 kJ/cm^2 and 10 μm focal position change for each repeat. The total number of lines for the two area scans is 200, and the total welded area size is 10 mm^2.

Figure 10 illustrates how the one-edge-sealed glass substrates are bonded together after laser processing; it shows the bottom glass is bonded together with the top glass sample when the top glass is held by tweezers.

After the one-edge sealing experiment, we further sealed a complete region by using four-edge sealing so as to protect the center region with or without optical coating on the surface. Two fused silica sample substrates without optical coatings were used to give a proof of concept demonstration. Figure 11 shows illustrations of the four-edge sealing of two fused silica samples with a USP laser; Fig. 11(a) shows the top view with interference fringe seen for those nonwelded regions and no interference fringe seen for those sealing seams, and Fig. 11(b) shows transmission view of the four welding seams crossing with each other with LED backlight illumination. Both of the sample dimensions are 10 mm × 10 mm with

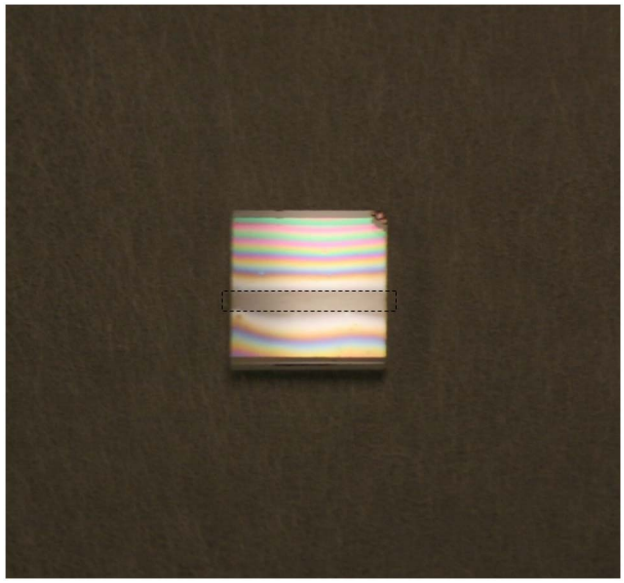

Fig. 9. (Color online) USP laser one-edge sealing with multi line welding the area without interference fringe is showing the welded region.

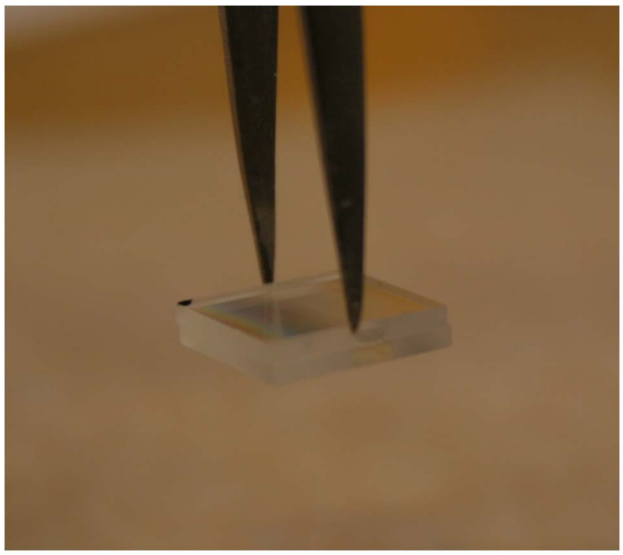

Fig. 10. (Color online) Bonded two substrates after USP laser one-edge sealing when holding the top glass sample by tweezers.

1.0 mm thickness. The welding speed is 1 mm/s and the average fluence used here is 26.5 kJ/cm^2. Scanning was repeated three times, with 10 μm focal position changes. For each sealing edge, the welded region area is 250 μm wide, so the welded seam area size is 2.5 mm^2 and the total welded area size for the four edges is 10 mm^2.

Figure 12 shows the microscopic top view of the sealing seams for the four-edge-sealed fused silica samples; Fig. 12(a) shows one of the sealing seams, comprised of multiple welding lines, and Fig. 12(b) shows one of the intersections of the two sealing seams. For all the welded regions, no interference fringe can be seen, while interference fringe can be seen for the nonwelded region.

To further show the hermetic sealing of the two substrates, one corner of the sealed sample was immersed in water to see whether or not water could penetrate the sealing seam. Figure 13 illustrates how the center region was well sealed by USP laser

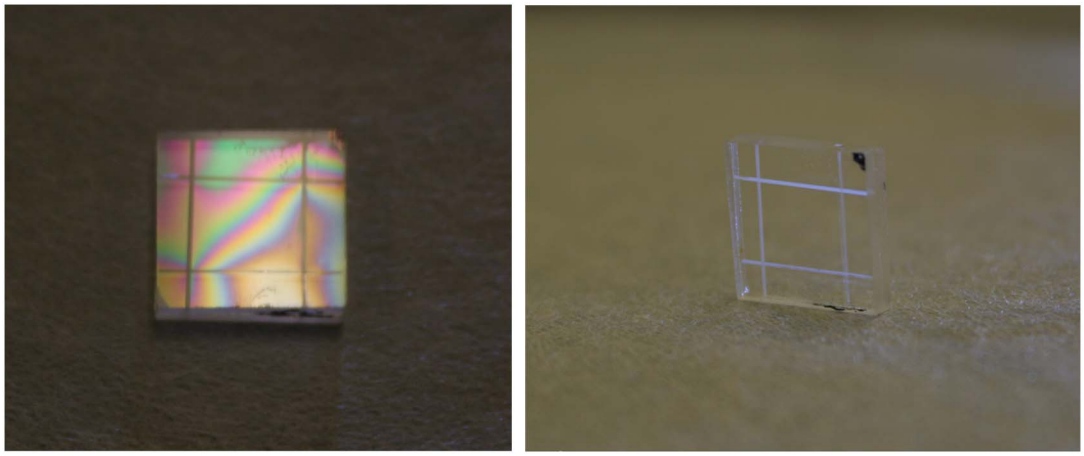

Fig. 11. (Color online) USP laser four-edge sealing of fused silica samples (F_{ave} = 26.5 kJ/cm^2): (a) top view with interference fringe seen for nonwelded regions and no interference fringe seen for those sealing seams, and (b) transmission view of the four welding seams crossing with each other with LED backlight illumination.

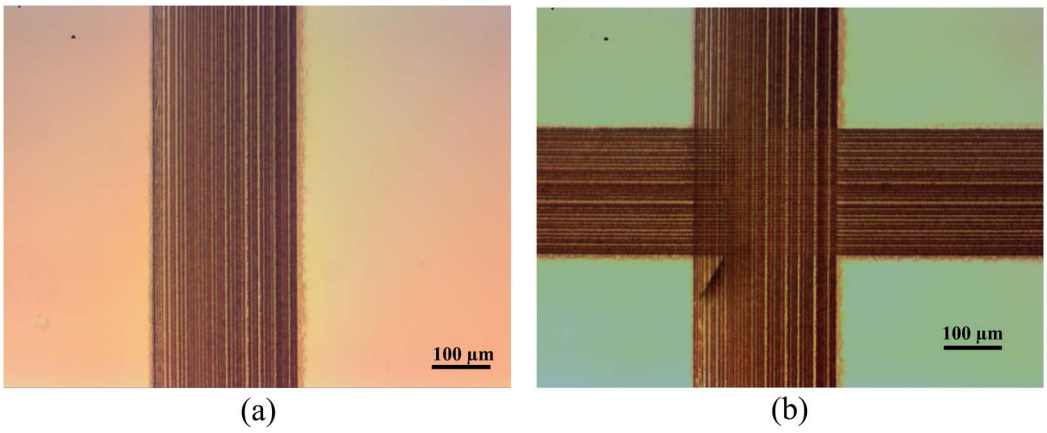

Fig. 12. (Color online) Microscopic view of USP laser four-edge sealing of two fused silica samples (F_{ave} = 26.5 kJ/cm^2): (a) one of the sealing seam composing of multiple welding lines, and (b) one of the intersections of two sealing seams.

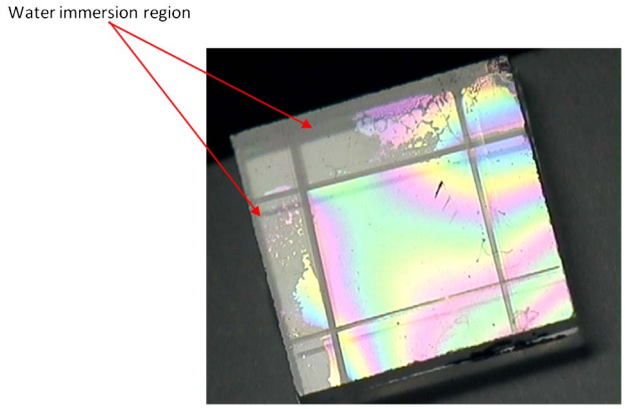

Fig. 13. (Color online) Camera view of the center region well sealed by USP laser-water immersion from top left corner cannot penetrate into the center region due to the block of sealed edges.

for a square-shaped sealing, and water immersion from the top left corner cannot penetrate into the center region due to the block of the surrounding sealing seams. The purpose of the sealing may not only be to contain a liquid, but also to seal against gas. Additionally, the bottom surface of the top glass substrate or the top surface of the bottom substrate may have coatings that are protected by the welding of a hermetically sealed region. The coating can be on one or both of the slides. The substrates can be comprised of any optically transparent substrate or filter that has a coating that needs to be protected from the environment. This enables the sealing of filters with coatings and even multilayer three-dimensional sealing of optically transparent materials for a variety of industrial applications.

4. Conclusion and Outlook

Welding and sealing of optically transparent materials using a USP fiber laser was demonstrated. Single line scanning-induced modification inside fused silica and single-line welding results, with different laser parameters, was studied at first. Then successful welding between fused silica with multiline scanning methods was investigated. To demonstrate proof of concept, complete four edge sealing of fused silica with USP laser repeat scanning was conducted. Further checks and a water immersion test confirmed the hermetic seal without voids or cracks. The joining process does not need any preprocessing before welding.

This work overcomes this limitation of small area welding and demonstrates the ability of USP lasers to weld and seal fused silica of a 10 mm^2 area. The capability of USP lasers to weld similar and dissimilar materials over a large area increases the potential for USP laser welding and sealing applications in the semiconductor industry, precision optics manufacturing, and aerospace engineering.

Future work on this patent pending process includes a welding stress evaluation and relationship study with laser processing parameters. Several methods have been proposed and can be used, such as a blade test [14] and push test [21]. Further work on higher pulse repetition rate and pulse energy, for faster welding speeds and high welding and sealing efficiency, is also necessary for potential applications in the semiconductor and optical assembly manufacturing industries.

This work was partially supported by the National Science Foundation (NSF), National Institute of Standards and Technology (NIST), and the U.S. Air Force Office of Scientific Research (AFOSR).

References

1. F. Niklaus, G. Stemme, J. Q. Lu, and R. Gutmann, "Adhesive wafer bonding," J. Appl. Phys. **99**, 031101 (2006).
2. V. Greco, F. Marchesini, and G. Molesini, "Optical contact and van der Waals interactions: the role of the surface topography in determining the bonding strength of thick glass plates," J. Opt. A **3**, 85–88 (2001).
3. M. Wild, A. Gillner, and R. Poprawe, "Locally selective bonding of silicon and glass with laser," Sens. Actuators A **93**, 63–69 (2001).
4. C. Yao, B. Xu, X. Zhang, J. Huang, J. Fu, and Y. Wu, "Interface microstructure and mechanical properties of laser welding copper-steel dissimilar joint," Opt. Lasers Eng. **47**, 807–814 (2009).
5. X. Cao and M. Jahazi, "Effect of welding speed on butt joint quality of Ti-6Al-4V alloy welded using a high-power Nd: YAG laser," Opt. Lasers Eng. **47**, 1231–1241 (2009).
6. A. Marcinkevičius, S. Juodkazis, M. Watanabe, M. Miwa, S. Matsuo, H. Misawa, and J. Nishii, "Femtosecond laser-assisted three-dimensional microfabrication in silica," Opt. Lett. **26**, 277–279 (2001).
7. H. Huang and Z. Guo, "Ultra-short pulsed laser PDMS thin-layer separation and micro-fabrication," J. Micromech. Microeng. **19**, 055007 (2009).
8. H. Huang and Z. Guo, "Human dermis separation via ultra-short pulsed laser plasma-mediated ablation," J. Phys. D **42**, 165204 (2009).
9. A. Y. Sajjadi, K. Mitra, and M. Grace, "Ablation of subsurface tumors using an ultra-short pulse laser," Opt. Lasers Eng. **49**, 451–456 (2010).
10. L. Shah, A. Arai, S. Eaton, and P. Herman, "Waveguide writing in fused silica with a femtosecond fiber laser at 522 nm and 1 MHz repetition rate," Opt. Express **13**, 1999–2006 (2005).
11. K. Miura, J. Qiu, H. Inouye, T. Mitsuyu, and K. Hirao, "Photo-written optical waveguides in various glasses with ultrashort pulse laser," Appl. Phys. Lett. **71**, 3329–3331 (1997).
12. S. Nolte, M. Will, J. Burghoff, and A. Tuennermann, "Femtosecond waveguide writing: a new avenue to three-dimensional integrated optics," Appl. Phys. A **77**, 109–111 (2003).
13. C. B. Schaffer, J. F. García, and E. Mazur, "Bulk heating of transparent materials using a high-repetition-rate femtosecond laser," Appl. Phys. A **76**, 351–354 (2003).
14. S. Richter, S. Döring, A. Tünnermann, and S. Nolte, "Bonding of glass with femtosecond laser pulses at high repetition rates," Appl. Phys. A **103**, 257–261 (2011).
15. W. Watanabe, S. Onda, T. Tamaki, and K. Itoh, "Direct joining of glass substrates by 1 kHz femtosecond laser pulses," Appl. Phys. B **87**, 85–89 (2007).
16. I. Miyamoto, A. Horn, J. Gottmann, D. Wortmann, and F. Yoshino, "Fusion welding of glass using femtosecond laser pulses with high-repetition rates," J. Laser Micro Nanoeng. **2**, 57–63 (2007).
17. S. Vukeli, P. Kongsuwan, and Y. L. Yao, "Ultrafast laser induced structural modification of fused silica—Part I: feature formation mechanisms," J. Manuf. Sci. Eng. **132**, 061012 (2010).

18. A. Horn, I. Mingareev, A. Werth, M. Kachel, and U. Brenk, "Investigations on ultrafast welding of glass—glass and glass—silicon," Appl. Phys. A **93**, 171–175 (2008).
19. T. Tamaki, W. Watanabe, and K. Itoh, "Laser micro-welding of transparent materials by a localized heat accumulation effect using a femtosecond fiber laser at 1558 nm," Opt. Express **14**, 10460–10468 (2006).
20. I. Miyamoto, A. Horn, and J. Gottmann, "Local melting of glass material and its application to direct fusion welding by ps-laser pulses," J. Laser Micro Nanoeng. **2**, 7–14 (2007).
21. K. Cvecek, I. Miyamoto, J. Strauss, M. Wolf, T. Frick, and M. Schmidt, "Sample preparation method for glass welding by ultrashort laser pulses yields higher seam strength," Appl. Opt. **50**, 1941–1944 (2011).
22. T. Tamaki, W. Watanabe, J. Nishii, and K. Itoh, "Welding of transparent materials using femtosecond laser pulses," Jpn. J. Appl. Phys. **44**, L687–L689 (2005).
23. W. Watanabe, S. Onda, T. Tamaki, K. Itoh, and J. Nishii, "Space-selective laser joining of dissimilar transparent materials using femtosecond laser pulses," Appl. Phys. Lett. **89**, 021106 (2006).